Analysis of nonlinear vibrations of a blade with dovetail attachment using DIC and the smoothed harmonics analysis

Analysis of nonlinear vibrations of a blade with dovetail attachment using DIC and the smoothed harmonics analysis

S. Occhipinti [1], **A. Cesaretti** [1], **P. Neri** [2], **C.M. Firrone** [1], **D. Botto** [1]
[1] Politecnico di Torino, Department of Mechanical Engineering,
Corso Duca Degli Abruzzi, 24, 10129 Torino, Italy

[2] University of Pisa, Department of Civil and Industrial Engineering,
Largo L. Lazzarino 2, 56122 Pisa, Italy

Abstract
This paper focuses on the experimental investigation of the effects of blade-root contact on turbine blade dynamics. Since under operating conditions the blade undergoes both cyclic loads and centrifugal loads, the nonlinear response of a dummy blade is investigated by means of a specially designed test rig, which allows tuning normal load and high-frequency excitation acting on the sample. To avoid interfering with the measurements, it is essential to avoid adding damping and external masses by attaching measuring instruments to the vibrating blade. Accordingly, Stereo Digital Image Correlation (Stereo-DIC) was used in this work to obtain full-field, non-contact measurements of specimen deformation. In this work, tests are performed exciting at a frequency higher than the maximum frame rate of the high-resolution cameras employed, and then a down-sampling technique, called Smoothed Harmonics Analysis (SHA), is implemented to avoid aliasing error in the detection of displacement signals.

1 Introduction

The study of the dynamic behavior of machine components is of paramount importance in many industrial fields. In particular, rotating machines are subject to dynamic loads that can cause fatigue failure if resonant conditions cannot be avoided. That is the reason why several service failures of gas turbine blades are due to high-cycle fatigue caused by large resonance stresses. Typical turbine disk assembly involves inserting the root of the blade inside the slot at the rim of the disc. Since there is relative motion between disk and blade, this type of joint affects the dynamics of the blade in terms of resonance frequencies and modal shapes. When excitation at resonance frequencies cannot be avoided in service, friction joints, that increase the mechanical damping, are used to reduce blade vibrations. Therefore, the design of bladed disks requires the prediction of their dynamic behavior. Thus, accurate dynamic models and dedicated experimental setups are needed to perform modal analysis, harmonic response analysis, and tests under full-scale operating conditions. Conventional experimental techniques using accelerometers and strain gauges produce point measurements. Consequently, when it is necessary to measure a significant number of degrees of freedom, the use of these devices may not be suitable. Full-field non-contact techniques can accelerate and improve the experimental task, as they avoid adding mass to the system and simplify the transmission of data for rotating machines. In this context, Scanning Laser Doppler Vibrometers (SLDV) stand out as one of the most established methods. Utilizing the Doppler effect, SLDV measures the velocity of a point on a specimen. Thus, by sweeping the laser beam across the surface through mirrors, [1], it facilitates measurements across multiple points. While SLDV enables highly accurate inspections of a specimen's surface, its primary drawback lies in the non-simultaneous acquisition of velocities at different points, resulting in a relative slow data acquisition process.

The rapid advancement of computer vision techniques has enabled the simultaneous measurement of spec-

imen surfaces at multiple points using digital cameras. Thus, the development of high-speed cameras has made these technique suitable for dynamic-field testing. In [2], the Motion Magnification algorithm was demonstrated to be effective for detecting structural damage on a wind turbine blade. Photogrammetry was utilized in [3] to measure the dynamic strain on a rotating three-bladed wind turbine. Additionally, the application of the Optical Flow technique was investigated and proven effective for experimental modal analysis, as shown in [4]. In this scenario, also Digital Image Correlation (DIC) demonstrated to be an alternative for dynamic-field testing, as discussed in [5]. In [6], DIC was utilized to achieve a comprehensive understanding of both the global and local motion of an underplatform damper. In [7], experimental parameter identification was conducted using full-field measurements from DIC, highlighting the advantages of utilizing full-field measurements over single-point measurements. However, cameras can only capture high-frequency phenomena at Nyquist frequencies by sacrificing image resolution, leading to reduced sensitivity of the measuring instrument. As a result, high-frame-rate camera systems may prove inadequate for applications involving the measurement of small displacements distributed over a large-scale structure. Moreover, the huge cost of high-speed cameras are unaffordable for many research centres. Various methodologies have been explored in the literature to enable high-resolution, low-speed cameras to accurately measure vibrations at high frequencies. These approaches involve setting the frame rate of the cameras below the Nyquist frequency of the analyzed motion and employing down-sampling techniques to prevent aliasing. In [8] a low-speed stereo-camera system was used to measure the modal shapes of a bladed disk. In this work the disk was sinusoidally forced at frequencies above the sampling frequency, overcoming the Nyquist-Shannon theorem by post-processing the DIC results using the Non-harmonic Fourier Analysis (NHFA). Another technique, used in [9], consists in acquiring pictures of a target during a periodic motion over several periods, in order to reconstruct the displacement signal in a period through a back-translation of samples.

The aim of this study is to measure the full-field high-frequency vibration of a mock-blade fixed with dovetail joints at both ends through a low-speed DIC system. The experimental task involves subjecting the blade to axial loading to simulate the centrifugal forces experienced by turbine blades during operational conditions. The measurement methodology employed involves post-processing the data obtained through the traditional 3D-DIC technique. 3D-DIC is implemented by capturing images of the mock-blade vibrating at high frequencies using standard high-resolution, low-speed cameras. Subsequently, the signal at each point of the blade is reconstructed using a down-sampling technique, called Smoothed Harmonics Analysis (SHA). This method ensures the correct reconstruction of the blade's deformed shape, effectively preventing aliasing errors.

2 Test Rig

Figure 1a illustrates the test rig used in this study. Given the challenges of managing a rotating test rig, the centrifugal force acting on the blade was simulated by applying a static axial load on it. The rig's symmetry is studied to guarantee equivalent loads and joint movements, making the outcomes directly comparable to those seen on a real blade. This was achieved by machining dovetail-type attachments at both ends of the blade, as shown in Fig. 1b, allowing to pull it without introducing extra damping. The specimen under consideration consists of a 26 mm x 10 mm rectangular-section beam with dovetail attachments at both ends. The overall length of the blade, inclusive of the dovetail extremities, measures 325.7 mm. Dovetail attachments slide into machined slots on two supports, each mounted on a crossbar. One support remains stationary while the other is linked to a manual pump. This pump applies axial force to the movable support through a hydraulic cylinder, allowing it to shift freely in the axial direction. The rig enables pressure readings on the hydraulic cylinder, allowing for the measurement of the applied axial force. Additionally, a full Wheatstone bridge of strain gauges attached to the beam provides a more precise measurement of the tensile load in the beam. For a deeper understanding of the rig's design principles refer to [10]. The mock-blade is excited at a point on its back surface, 15 mm from the rig's fixed support, using an electrodynamic shaker. The shaker is connected to the beam through a stinger, which is linked to a load cell attached to the beam. A waveform generator produces a sinusoidal excitation at a frequency near the blade's resonance, which is then amplified by a power amplifier connected to the shaker. A Laser Doppler Vibrometer (LDV) measures the velocity at a reference point on the blade's back surface. Strain gauges, load cell and LDV

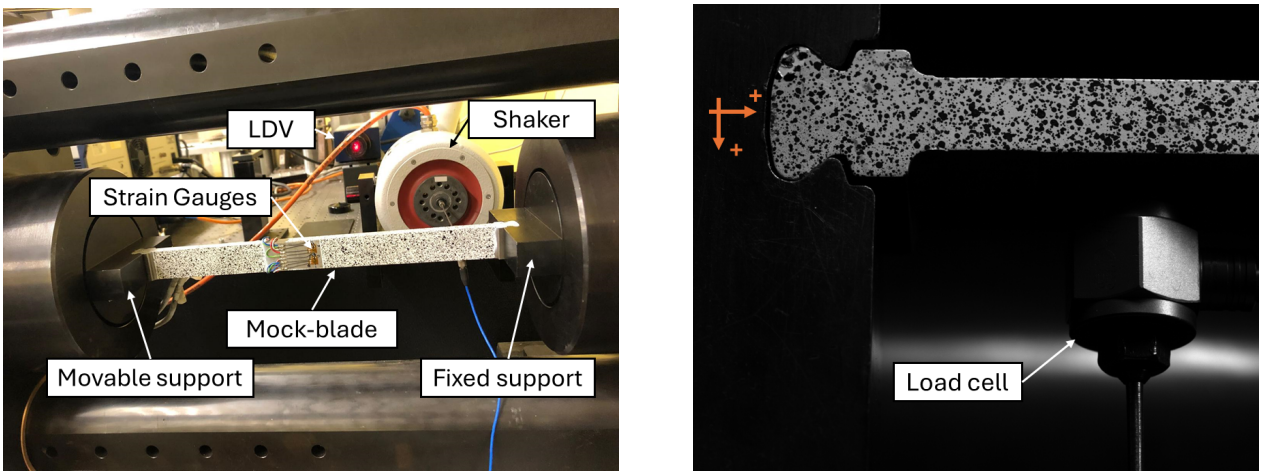

(a) (b)

Figure 1: (a) Test rig: A mock-blade is fixed at both ends to two supports, with one support fixed and the other movable via a hand pump. (b) Close-up of the dovetail attachment at one end of the blade and its support. It is also shown the point of excitation by the stinger connected to the shaker. The sign convention used to plot displacement signals is represented in orange.

signals are recorded by a Data Acquisition (DAQ) system.

However, plotting the displacement maps of the blade using only these measurement devices is not possible without making assumptions about its deformed shapes, as they provide information only at single points. Indeed, utilizing multiple strain gauges or LDVs to obtain synchronous information on the blade surface dynamics could lead to an expensive setup or interfere with the specimen dynamics by adding external damping and mass. DIC allows performing a full-field analysis of the blade, overcoming the limitations of the others measurement device. Given the limitation of high-speed cameras in terms of cost and sensor resolution, the motion of the blade's front surface was measured using a low-speed 3D-DIC system, shown in Fig. 2a. This system comprises two Optomotive Spinosaurus cameras, each equipped with a 23 MP Fujinon lens with a 35 mm focal length. These cameras feature high-resolution sensors capable of recording 7.1 MP images at a maximum frame rate of 200 fps and with a minimum shutter time of 2 µs. In order to avoid blurred images high-intensity illumination is needed to compensate for the loss of image brightness caused by a shorter shutter time. Thus, two 200 W Stratus LED modules were used to illuminate the blade surface. The data acquisition was initiated for all measurement devices by a common trigger signal, providing a common time reference for all measured signals.

3 Measurement Process

Predicting the motion of structures with interfaces is challenging because the tangential force depends on the state of the contact (stick, slip, or separation). When the contact is in a stick state, the structure can be considered linear. On the contrary, non-linearities arise from the friction at the blade roots due to the relative motion between the blade and supports. Therefore, the response of the blade, also to a given single harmonic excitation, strongly depends on the applied axial load (centrifugal load in real blades) and the amplitude of the excitation. Experimental tests to predict the resonance frequency of the tested mock-blade were performed in [11]. In these tests, the free decay of the blade, pulled with different axial load and excited using a method called the Detached Drive Rod Method, was measured with a Laser Doppler Vibrometer (LDV). In the present work, these results were used to predict the resonance frequency of the blade at different loading conditions.

The displacement of the blade's front surface was recorded thought 3D-DIC technique. DIC analysis requires a unique pattern for the pixel subsets representing points on the sample surface, thus, a speckle pattern was

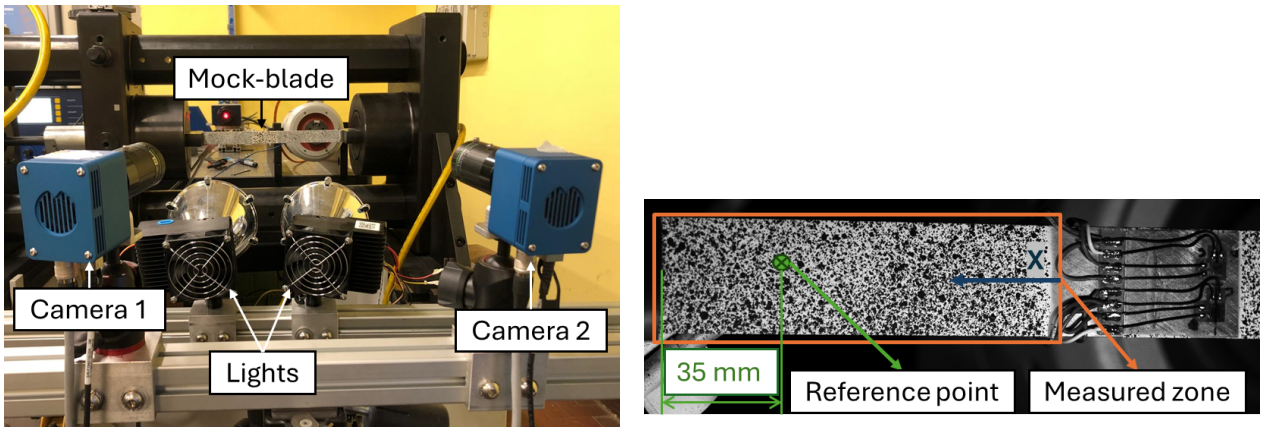

(a) (b)

Figure 2: (a) 3D-DIC setup with two low-speed cameras and high-power LED lights to measure the motion of the speckled surface of the blade. (b) Measured area of the blade: the position of the reference point (corresponding to that measured by LDV on the rear side of the blade) is highlighted. The x-axis shown defines the convention used to plot deformed shapes.

applied to the blade surface. This pattern was generated by applying a base coat of white paint and then spraying black speckles. Images were acquired using an exposure time of 5 µs and camera's full resolution. The frame rate of the cameras was set to meet the requirements of the downsampling technique, as explained in Section3.2. High sensitivity is crucial for accurately capturing the non-linear behavior of the beam. Since the sensitivity of the DIC technique is closely related to the image scale (it can be estimated as 1/100 of the pixel size), tests were performed with a reduced image scale to enhance measurement accuracy. To achieve this, only half of the beam, from the center to the movable support, was recorded. By doing so, and given the symmetry of the rig, no relevant information on the blade operative shapes was lost, while the accuracy of the measurement device was enhanced. It results in high-quality images of the blade with a scale of around 0.1 mm/pixel. However, the presence of strain gauges complicates DIC measurement in the central zone of the beam, limiting the DIC measurements to the area highlighted in Fig. 2b. The out-of-plane vibration of the blade was recorded through an high-frequency laser vibrometer (LDV) on a reference point of the blade, located 35 mm from the movable support.

3.1 Stereo Digital Image Correlation

The core of a stereo-Digital Image Correlation (stereo-DIC) algorithm involves processing images captured from different perspectives through DIC algorithm. It involves tracking the displacement and deformation of the sample surface by analyzing changes in the position and shape of recorded patterns over time. In this work, Ncorr [12], an open-source Matlab program, was used. Another crucial step in a stereo-DIC program is calibrating the stereo-camera system. Calibration for each camera in a stereo pair aims to determine the transformation that maps each image point on camera sensors to its corresponding 3D point in the global coordinate system, following the pinhole optical model, see [13]. In this work, the calibration was performed using the MATLAB Stereo Camera Calibrator App [14]. Once the positions of the subsets are defined in the frames of both cameras and with an established stereo-camera model, it becomes possible to triangulate the positions of each point. This makes it possible to calculate the spatial position of points in time, thus deriving the displacement and deformation fields.

3.2 Smoothed Harmonic Analysis

The DIC algorithm can compute displacement maps only at the specific times defined by the camera's timestamps. However, the maximum frame rate of the cameras used is much slower than the sampling rate needed

to accurately capture the response near the first bending resonance. To address this, a downsampling method called Smoothed Harmonic Analysis (SHA) was used, see [15]. SHA leverages on the capability to extract information about a period of a periodic signal by sampling at a rate below its Nyquist frequency (i.e., downsampling) across various periods. The SHA method is briefly described below. The method starts from the well-known fact that a signal with a finite number m of relevant harmonic contributions, denoted as y, can be approximated as a combination of sine and cosine functions using the Fourier series.

$$y(t) \approx (1 \ \ldots \ \cos(\omega_j t) \ \sin(\omega_j t) \ \ldots \ \cos(\omega_m) \ \sin(\omega_m t)) \begin{pmatrix} A_0 \\ \vdots \\ A_j \\ B_j \\ \vdots \\ A_m \\ B_m \end{pmatrix} = \mathbf{p}^\intercal \cdot \mathbf{q} \tag{1}$$

where t represents the time variable in which the signal is defined, ω_j is the *j*th harmonic frequency and A_j and B_j are the amplitudes of the cosine and sine components, respectively. If the frequencies ω_j of the main harmonics on the signal spectrum are known, the vector $\mathbf{p}$, containing the harmonic waves, is known, while the vector $\mathbf{q}$, containing the amplitude of each wave, remains unknown. Eq. 1 could be written at all the sampling time. Hence, if the signal y is known at a large number n of time instants, i.e., if enough samples were acquired, it yields an overdetermined system:

$$\begin{Bmatrix} y_{(t_1)} \\ \vdots \\ y_{(t_i)} \\ \vdots \\ y_{(t_n)} \end{Bmatrix} \approx \begin{bmatrix} 1 & \ldots & \cos(w_j t_1) & \sin(w_j t_1) & \ldots & \cos(w_m t_1) & \sin(w_m t_1) \\ & & & \vdots & & & \\ 1 & \ldots & \cos(w_j t_i) & \sin(w_j t_i) & \ldots & \cos(w_m t_i) & \sin(w_m t_i) \\ & & & \vdots & & & \\ 1 & \ldots & \cos(w_j t_n) & \sin(w_j t_n) & \ldots & \cos(w_m t_n) & \sin(w_m t_n) \end{bmatrix} \cdot \begin{pmatrix} A_0 \\ \vdots \\ A_j \\ B_j \\ \vdots \\ A_m \\ B_m \end{pmatrix} \tag{2}$$

This system can be solved using the least squares method to find the vector $\mathbf{q}$, thereby enabling the computation of the spectrum of y and the reconstruction of the signal in time. The goodness of this process is addressed by two requirements. Firstly, the signal main harmonics must be known. In experimental mechanics, predicting the relevant frequencies of a linear system's response is straightforward when the excitation frequency is known, as linear systems vibrate at the same frequencies as the excitation. This scenario typically occurs in laboratory conditions where a well-known force excites a structure. For nonlinear system, whose response to even a controlled single harmonic excitation can be unpredictable, it is not true. However, the response spectrum of a nonlinear structure to a single harmonic excitation is often related to the excitation frequency, as it contains sub-harmonics and super-harmonics of the excitation frequency. This requirement can be verified by measuring the response with a high sampling rate single point measurement device, such as an accelerometer or LDV. Therefore, the downsampled response can be accurately reconstructed by considering the harmonics at multiples and submultiples of the excitation frequency. The other requirement is related to the sampling acquisition itself. Given that the SHA method relies on least squares fitting, the acquired samples must contain precise information about the signal period. When the sampling period T_s aligns as a multiple of the signal period T_v, the algorithm samples the same signal point at different intervals, leading to redundancy of information within the period. Consequently, this redundancy can result in poor information for the algorithm. Although infinite combinations of sampling frequency f_s and the number of samples n can result in suitable signal sampling, a relationship between them that optimizes the sampling

time can be written as

$$f_s = \frac{1}{T_s} = \frac{1}{kT_v + \Delta t} \tag{3a}$$

$$n = \frac{T_v}{\Delta t} \tag{3b}$$

Here, k and Δt have to be set based on the maximum speed of the measurement device and the highest frequency of the signal. Specifically, k controls how many samples per period will be acquired, and Δt is the time resolution with which we are sampling the signal period, thus linked to the Nyquist frequency of the signal. For more details, see [15].

4 Results

Strain gauges, LDV, and cameras were used to analyze the blade motion. Tests were performed under two different axial loading conditions, with purely sinusoidal excitation near the corresponding first bending mode resonances:

- Firstly, the blade was subjected to a 24 kN axial load and excited at 541 Hz. In this test, the contact remained in a stick state, and the structure could be considered linear.
- Then, the blade was subjected to a 1 kN axial load and excited at 480 Hz. The lower resonance frequency (and thus the selected excitation frequency) is due to the decreased stiffness of the structure resulting from the lower axial load.

The presence of superharmonics of the excitation arising from nonlinearities was considered up to the fifth order during the setting of sampling parameters, resulting in Nyquist frequencies of signals close to 6 kHz. Strain gauges and LDV were set to record at 50 kHz, thereby largely satisfying the Nyquist-Shannon requirement during both tests. Since the maximum frame rate of the employed cameras was 200 Hz, a downsampling approach coupled with SHA was used for DIC analysis. Thus, according to the downsampling approach, see 3.2:

- 55 frames of the blade motion under a 24 kN axial load were acquired at 76.8 Hz;
- 55 frames of the blade motion under a 1 kN axial load were acquired at 68.7 Hz.

Figure 3 shows the displacement signals of the reference point on the blade measured during the two tests. Signals recorded by the DIC and SHA methods, are overlapped with the displacement signal recorded by the laser, to evaluate the accuracy of the signal reconstruction process for both test. Only one relevant harmonic was found in the blade response when it was pulled at 24 kN, confirming the linear behaviour. However, during the 1 kN test, the relative motion between the blade and supports caused nonlinearities to arise. These nonlinearities were evidenced by the relevant contribution of the first two odd superharmonics of the excitation to the blade response. To highlight the nonlinearities, the displacement data obtained from DIC and SHA were derived in time to obtain the velocity of the reference point during the two tests. The results in terms of velocity are plotted in Fig. 4, overlapped with the LDV velocity signal recorded at the same reference point. In the same figure, the main harmonics of signals are compared in bar plots, revealing the good accuracy of the SHA method in identifying harmonic contributions. The observed discrepancies are reasonable given that both laser and camera measurements are subject to inevitable misalignments and disturbances, and that measuring the same point on two different surfaces is challenging. It is also noticeable that even though the acquisition by cameras and LDV was synchronized by a common trigger signal, the sample acquisition process is governed by the devices' internal clocks, leading to a delay between DIC and LDV signals. By iterating this process for all the measured points, employing DIC and the SHA method enables the plotting of the deformation of the measured portion of the blade. Fig. 5 shows the measured deformed shape of the blade at the time of maximum deformation during the two tests. For plotting the results, displacement data were extracted for points along the axial symmetry axis of the blade (x-axis in Fig. 2b).

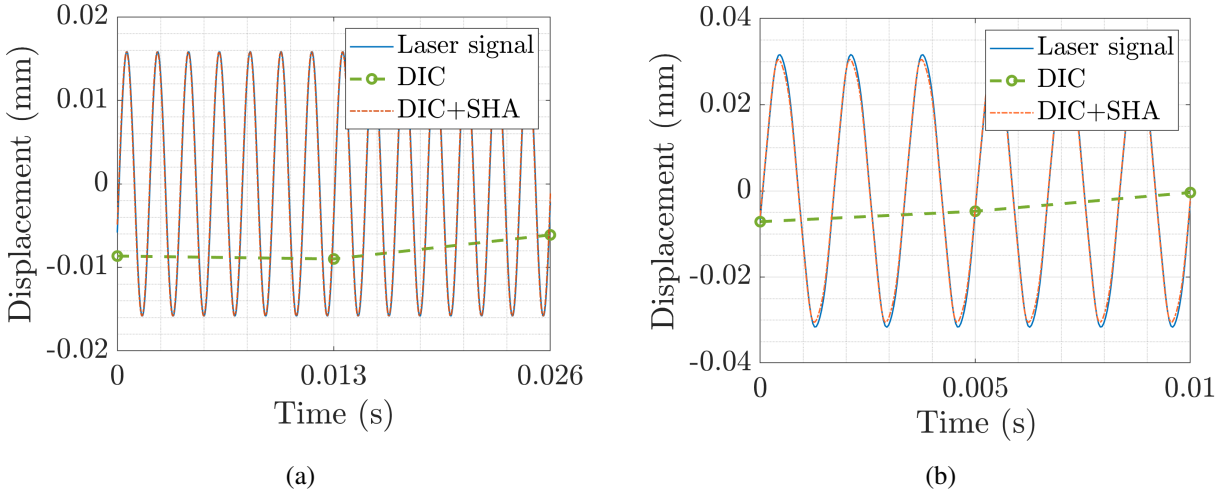

Figure 3: Displacement signals measured at a reference point on the blade under (a) 24 kN axial force and (b) 1 kN axial force. Signals were measured using LDV (blue), DIC (green), and the SHA method applied to DIC samples (red).

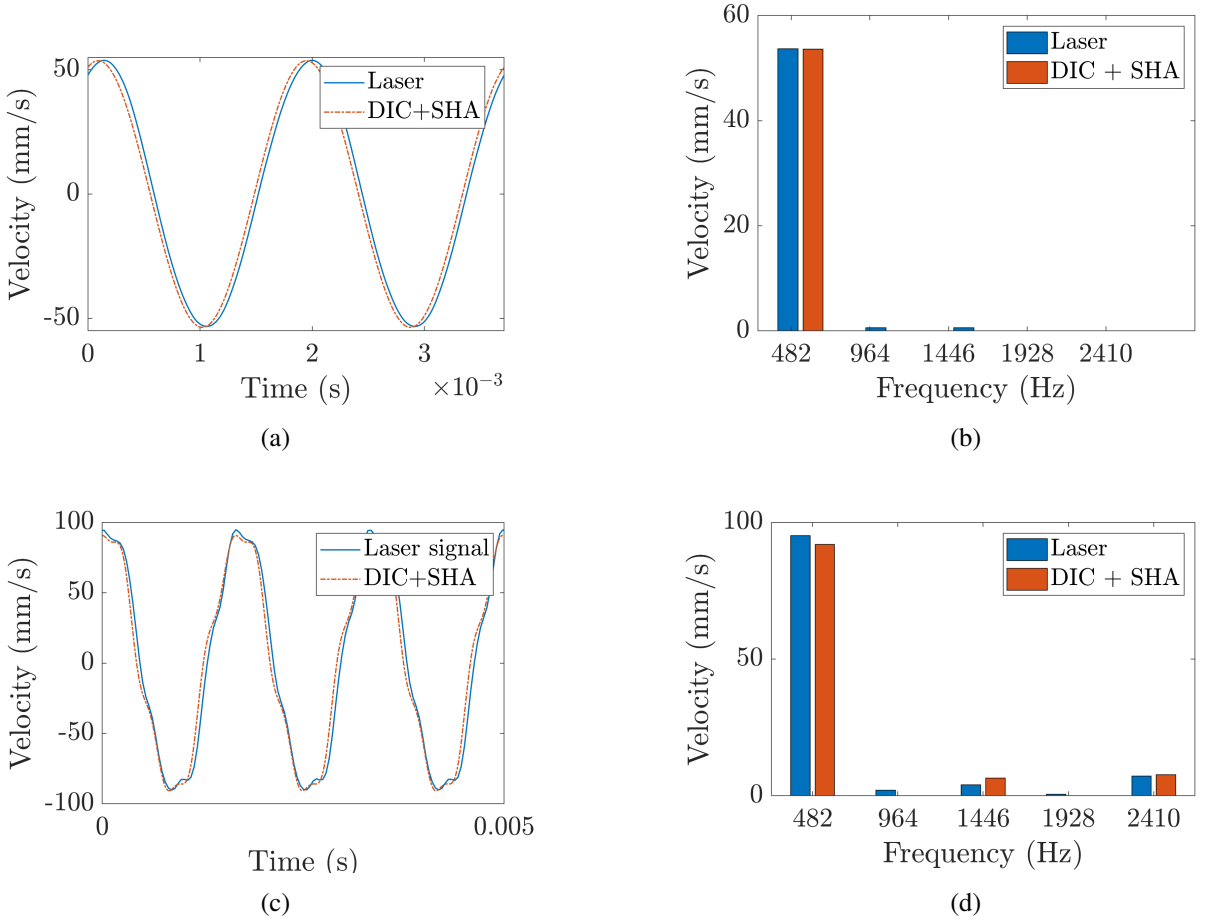

Figure 4: Velocity signals measured at a reference point on the blade under (a-b) 1 kN and (c-d) 24 kN axial forces using LDV (blue) and the SHA method applied to DIC (red). The signals are presented in the time domain (a, c). In the frequency domain plots (b, d), main harmonics of the signals are compared in bar plots.

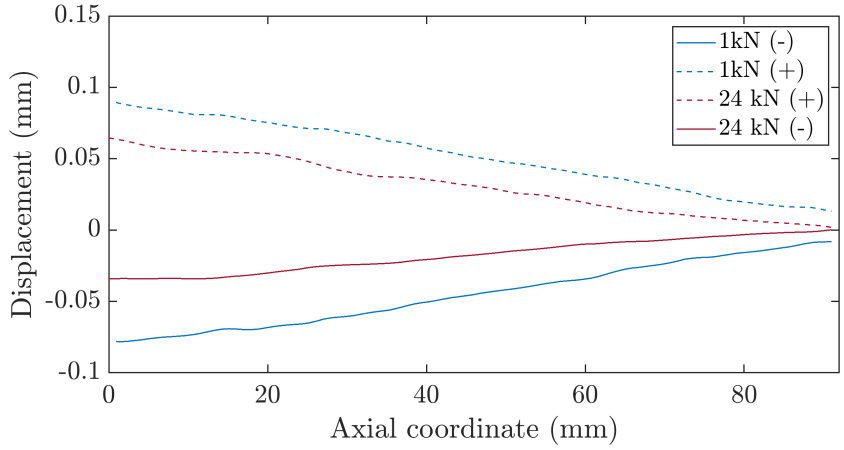

Figure 5: Deformed shapes of the blade recorded in the measured area by DIC and SHA during the 1 kN normal load test (in blue) and the 24 kN normal load test (in red). Dotted lines represent the deformed shape in the positive direction, while continuous lines represent the deformed shape in the negative direction, following the sign convention for displacement depicted in Fig. 1b. The points used for plotting lie on the axial symmetry axis of the blade, as defined in Fig. 2b.

5 Conclusion

In this paper, the high-frequency motion of a mock-blade was analyzed using a specially designed rig. To simulate the centrifugal forces experienced by turbine blades during operational conditions, the blade was subjected to a normal load. Subsequently, it was excited close to its first bending resonance frequency, which strongly depends on the normal load. Strain gauges were attached to the blade surface to measure the normal load. The testing involved two loading conditions: initially, under a 24 kN axial load and excitation at 541 Hz, followed by a test with a 1 kN axial load and dynamic excitation at 480 Hz. Analysis of a portion of the blade was conducted using a low-frequency 3D-Digital Image Correlation (DIC) setup, employing a downsampling approach known as Smoothed Harmonics Analysis (SHA). The DIC maximum sampling rate is approximately 200 Hz. Consequently, the cameras were configured to record at frequencies significantly lower than the Nyquist frequency of the systems, which were found to be over 1 kHz for the first test and even higher for the second one, where superharmonic components arose (making the system Nyquist frequency exceeds 6 kHz). To reconstruct the downsampled responses measured by DIC and avoid aliasing, it is necessary for the system responses to exhibit periodic behavior, with knowledge of the main harmonic frequencies of the blade responses. To verify the periodicity of the response, the motion of a reference point on the blade was accurately measured using a Laser Doppler Vibrometer (LDV). The main harmonics of the signals were sought among the superharmonics of the excitation frequency, as it is common for nonlinear systems to exhibit superharmonic components in their response. LDV measurements confirmed the main frequencies in the response spectra, enabling an accurate reconstruction of DIC downsampled signals. Thus, DIC technique allows for plotting the deformed shape of nearly half of the blade, results that are not achievable with conventional measurement instruments without interfering with the blade dynamics. Moreover, the methodology used proves to be effective for high-resolution analysis of high-frequency dynamics, overcoming the limitations of high-speed cameras, which are characterized by relatively low resolution and high cost. The measurements performed here are useful for characterizing blade dynamics under different loading conditions. However, strain gauges interfered with the full-field measurement by decreasing the measurable area. To improve the dynamic characterization of the blade in future works, strain gauges can be replaced by high-resolution DIC, performed in a small area of the blade to achieve the necessary high sensitivity.

References

[1] B. Halkon and S. Rothberg, "Vibration measurements using continuous scanning laser vibrometry: Advanced aspects in rotor applications," *Mech Syst Signal Pr*, vol. 20, no. 6, pp. 1286–1299, aug 2006.

[2] A. Sarrafi, Z. Mao, C. Niezrecki, and P. Poozesh, "Vibration-based damage detection in wind turbine blades using phase-based motion estimation and motion magnification," *Journal of Sound and Vibration*, vol. 421, pp. 300–318, May 2018.

[3] J. Baqersad, P. Poozesh, C. Niezrecki, and P. Avitabile, "A noncontacting approach for full-field strain monitoring of rotating structures," *Journal of Vibration and Acoustics*, vol. 138, no. 3, Apr. 2016.

[4] J. Javh, J. Slavič, and M. Boltežar, "The subpixel resolution of optical-flow-based modal analysis," *Mechanical Systems and Signal Processing*, vol. 88, pp. 89–99, May 2017.

[5] A. J. Molina Viedma, L. Felipe-Sesé, E. López-Alba, and F. A. Díaz, "Comparative of conventional and alternative digital image correlation techniques for 3d modal characterisation," *Measurement*, vol. 151, p. 107101, Feb. 2020.

[6] L. Pesaresi, M. Stender, V. Ruffini, and C. W. Schwingshackl, "DIC measurement of the kinematics of a friction damper for turbine applications," in *Dynamics of Coupled Structures, Volume 4*. Springer International Publishing, 2017, pp. 93–101.

[7] K. Zaletelj, J. Slavič, and M. Boltežar, "Full-field dic-based model updating for localized parameter identification," *Mechanical Systems and Signal Processing*, vol. 164, p. 108287, Feb. 2022.

[8] P. Neri, A. Paoli, A. V. Razionale, and C. Santus, "Low-speed cameras system for 3d-DIC vibration measurements in the kHz range," *Mech Syst Signal Pr*, vol. 162, p. 108040, jan 2022.

[9] M. T. Endo, A. N. Montagnoli, and R. Nicoletti, "Measurement of shaft orbits with photographic images and sub-sampling technique," *Exp Mech*, vol. 55, no. 2, pp. 471–481, sep 2014.

[10] M. Allara, S. Filippi, and M. M. Gola, "An experimental method for the measurement of blade-root damping," in *Volume 5: Marine; Microturbines and Small Turbomachinery; Oil and Gas Applications; Structures and Dynamics, Parts A and B*, ser. GT2006. ASMEDC, Jan. 2006.

[11] D. Botto, M. Glorioso, S. Occhipinti, and F. Cuccovillo, "Uncertainty in identifying contact stiffness in a dovetail attachment for turbine blades," *Mechanical Systems and Signal Processing*, vol. 197, p. 110379, Aug. 2023.

[12] J. Blaber, B. Adair, and A. Antoniou, "Ncorr: Open-source 2d digital image correlation matlab software," *Experimental Mechanics*, vol. 55, no. 6, pp. 1105–1122, Mar. 2015.

[13] R. Hartley and A. Zisserman, *Multiple View Geometry in Computer Vision*. Cambridge University Press, Mar. 2004.

[14] T. M. Inc., "Computer vision toolbox," Natick, Massachusetts, United States, 2023. [Online]. Available: https://www.mathworks.com

[15] S. Occhipinti, P. Neri, C. M. Firrone, and D. Botto, *Analysis of Nonlinear Vibrations Using DIC and the Smoothed Harmonics Method*. Springer Nature Switzerland, 2024, pp. 691–701.